5.2.2.2 Highly Dispersed Ruthenium on Titania

In an attempt to further investigate the hydrocarbon cutoff hypothesis ruthenium Catalyst 5345-61 (0.93 wt.% Ru) was prepared on titania (anatase) by a conventional aqueous impregnation. Ruthenium particles were not observed during the STEM examination, indicating that the ruthenium particles were smaller than 2 nm. Before the test, the ruthenium catalyst on titania was heated under H_2 flow at 1 atm to 600°C, and maintained at that temperature for 2 hours in order to achieve strong-metal-support interaction. The catalyst was then cooled to 208°C for a pressure test at 49 atm with He followed by introducion of synthesis gas at 35 atm.

Catalyst 5345-61 was tested at 208°C, 35 atm, H_2:CO feed ratio = 2, GHSV 460 hr^{-1} for 12 hours in Run 30.

The space velocity was higher with the titania-supported highly dispersed ruthenium catalyst relative to the alumina-supported highly dispersed ruthenium catalyst tested in Run 25 partly because the titania support was about three times denser than alumina.

The test duration in Run 30 was kept short in order to minimize ruthenium metal agglomeration. An earlier run (29) with the same catalyst showed the catalyst's maximum temperature to become uncontrollably high. γ-Al_2O_3 powder was therefore used in Run 30 to dilute the catalyst bed and to control the bed temperature.

The results obtained in Run 30 are summarized in Tables 5-37 and 5-38 and Figures 5-220 through 5-226.

The CO conversion declined from 45% at 2 hours on stream to 7.5% by the end of the 12-hour-test (Figure 5-220). The CO selectivity to CO_2 was about 5% for most of the run, apparently indicating minimal water gas shift activity,

Table 5-37. Product Distributions in Run 30

WEIGHT PCTS WITHOUT ARGON	
HYDROGEN	9.888
CARBON MONOXIDE	68.077
CARBON DIOXIDE	1.536
WATER	14.050
HYDROCARBONS	6.208
OXYGENATES	0.242
HYDROCARBON DISTRIBUTION	
C1	5.841
C2 - C4	13.283
C5 - C11	25.524
C12 - C18	6.560
C19 - C25	0.946
C26 PLUS	47.847
C1 - C44	52.153
C45 PLUS	47.847
OXYGENATES DISTRIBUTION	
ALCOHOLS	100.000
ALDEHYDES	0.000
OTHER OXYGENATES	0.000
MOLE PCTS WITHOUT ARGON	
HYDROGEN	59.697
CARRON MONOXIDE	29.583
CARBON DIOXIDE	0.425
WATER	9.493
HYDROCARBONS	0.740
OXYGENATES	0.061
RECOVERIES	
OVERALL	91.937
CARBON	86.150
HYDROGEN	90.442
OXYGEN	97.214
ARGON	90.572
CORRECTED RECOVERIES	
OVERALL	101.507
CARBON	95.117
HYDROGEN	99.856
OXYGEN	107.333

HYDROGEN	9.8875
CARBON MONOXIDE	68.0773
CARBON DIOXIDE	1.5356
METHANE	0.3626
ETHANE	0.0897
ETHYLENE	0.0000
PROPANE	0.1148
PROPYLENE	0.1904
BUTANE	0.1465
BUTENE	0.2833
AQUEOUS ANALYSIS, WT%	
WATER	14.0499
ALCOHOLS	
C1	0.0611
C2	0.0936
C3	0.0117
C4	0.0377
C5	0.0260
C6	0.0117
C7	0.0000
C8	0.0000
C9	0.0000
C10	0.0000
ALDEHYDES	
C1	0.0000
C2	0.0000
C3	0.0000
C4	0.0000
C5	0.0000
C6	0.0000
C7	0.0000
C8	0.0000
C9	0.0000
C10	0.0000
OTHER OXYGENATES	
C1	0.0000
C2	0.0000
C3	0.0000
C4	0.0000
C5	0.0000
C6	0.0000
C7	0.0000
C8	0.0000
C9	0.0000
C10	0.0000

Table 5-38. Hydrocarbon Distributions in Run 30

C1	5.8406	C51	1.1108	C101	0.2777	C151	0.0781	C201	0.0222
C2	1.4448	C52	1.0581	C102	0.2708	C152	0.0761	C202	0.0217
C3	4.9163	C53	1.0250	C103	0.2640	C153	0.0742	C203	0.0211
C4	6.9223	C54	0.9935	C104	0.2573	C154	0.0723	C204	0.0205
C5	3.9280	C55	0.9830	C105	0.2507	C155	0.0705	C205	0.0200
C6	3.1315	C56	0.9543	C106	0.2432	C156	0.0687	C206	0.0194
C7	5.4465	C57	0.9267	C107	0.2368	C157	0.0670	C207	0.0170
C8	4.6093	C58	0.9002	C108	0.2305	C158	0.0653	C208	0.0165
C9	3.6752	C59	0.8758	C109	0.2243	C159	0.0622	C209	0.0160
C10	2.5759	C60	0.8512	C110	0.2182	C160	0.0607	C210	0.0155
C11	2.1572	C61	0.8273	C111	0.2123	C161	0.0592	C211	0.0151
C12	1.5739	C62	0.8044	C112	0.2065	C162	0.0578	C212	0.0146
C13	1.2878	C63	0.7711	C113	0.2009	C163	0.0564	C213	0.0142
C14	1.2437	C64	0.7497	C114	0.1955	C164	0.0550	C214	0.0137
C15	1.0677	C65	0.7290	C115	0.1891	C165	0.0537	C215	0.0133
C16	0.6162	C66	0.7090	C116	0.1841	C166	0.0525	C216	0.0129
C17	0.4402	C67	0.6895	C117	0.1793	C167	0.0512	C217	0.0125
C18	0.3301	C68	0.6781	C118	0.1746	C168	0.0500	C218	0.0121
C19	0.2421	C69	0.6596	C119	0.1701	C169	0.0489	C219	0.0117
C20	0.1761	C70	0.6416	C120	0.1658	C170	0.0478	C220	0.0113
C21	0.1321	C71	0.6242	C121	0.1616	C171	0.0467	C221	0.0109
C22	0.1100	C72	0.6073	C122	0.1576	C172	0.0456	C222	0.0106
C23	0.1321	C73	0.5854	C123	0.1536	C173	0.0453	C223	0.0103
C24	0.0660	C74	0.5696	C124	0.1507	C174	0.0442	C224	0.0099
C25	0.0880	C75	0.5544	C125	0.1470	C175	0.0432	C225	0.0096
C26	0.0000	C76	0.5395	C126	0.1434	C176	0.0422	C226	0.0093
C27	0.0000	C77	0.5251	C127	0.1398	C177	0.0412	C227	0.0089
C28	0.0000	C78	0.5127	C128	0.1364	C178	0.0402	C228	0.0086
C29	0.0000	C79	0.4990	C129	0.1331	C179	0.0392	C229	0.0084
C30	0.0000	C80	0.4857	C130	0.1298	C180	0.0383	C230	0.0081
C31	0.0000	C81	0.4726	C131	0.1267	C181	0.0373	C231	0.0079
C32	0.0000	C82	0.4598	C132	0.1236	C182	0.0364	C232	0.0077
C33	0.0000	C83	0.4474	C133	0.1206	C183	0.0355	C233	0.0075
C34	0.0000	C84	0.4376	C134	0.1177	C184	0.0347	C234	0.0073
C35	0.0000	C85	0.4256	C135	0.1140	C185	0.0338	C235	0.0071
C36	0.0000	C86	0.4139	C136	0.1112	C186	0.0330	C236	0.0069
C37	0.0000	C87	0.4024	C137	0.1086	C187	0.0321	C237	0.0067
C38	0.0000	C88	0.3913	C138	0.1060	C188	0.0313	C238	0.0066
C39	0.0000	C89	0.3806	C139	0.1034	C189	0.0303	C239	0.0064
C40	0.0000	C90	0.3702	C140	0.1010	C190	0.0295	C240	0.0063
C41	0.0000	C91	0.3544	C141	0.0985	C191	0.0288	C241	0.0061
C42	0.0000	C92	0.3449	C142	0.0962	C192	0.0281	C242	0.0060
C43	0.0000	C93	0.3357	C143	0.0939	C193	0.0274	C243	0.0059
C44	0.0000	C94	0.3269	C144	0.0916	C194	0.0267	C244	0.0057
C45	1.3327	C95	0.3184	C145	0.0893	C195	0.0260	C245	0.0056
C46	1.2855	C96	0.3102	C146	0.0886	C196	0.0253	C246	0.0055
C47	1.2407	C97	0.3023	C147	0.0864	C197	0.0247	C247	0.0053
C48	1.2271	C98	0.2996	C148	0.0843	C198	0.0241	C248	0.0052
C49	1.1864	C99	0.2921	C149	0.0822	C199	0.0234	C249	0.0052
C50	1.1476	C100	0.2848	C150	0.0801	C200	0.0228	C250	0.0051

Figure 5-220. Titania-Supported Highly Dispersed Ruthenium Catalyst 5345-61; Conversions in Run 30 (H_2:CO Feed Ratio = 2.0, 208°C at Inlet, 35 atm)

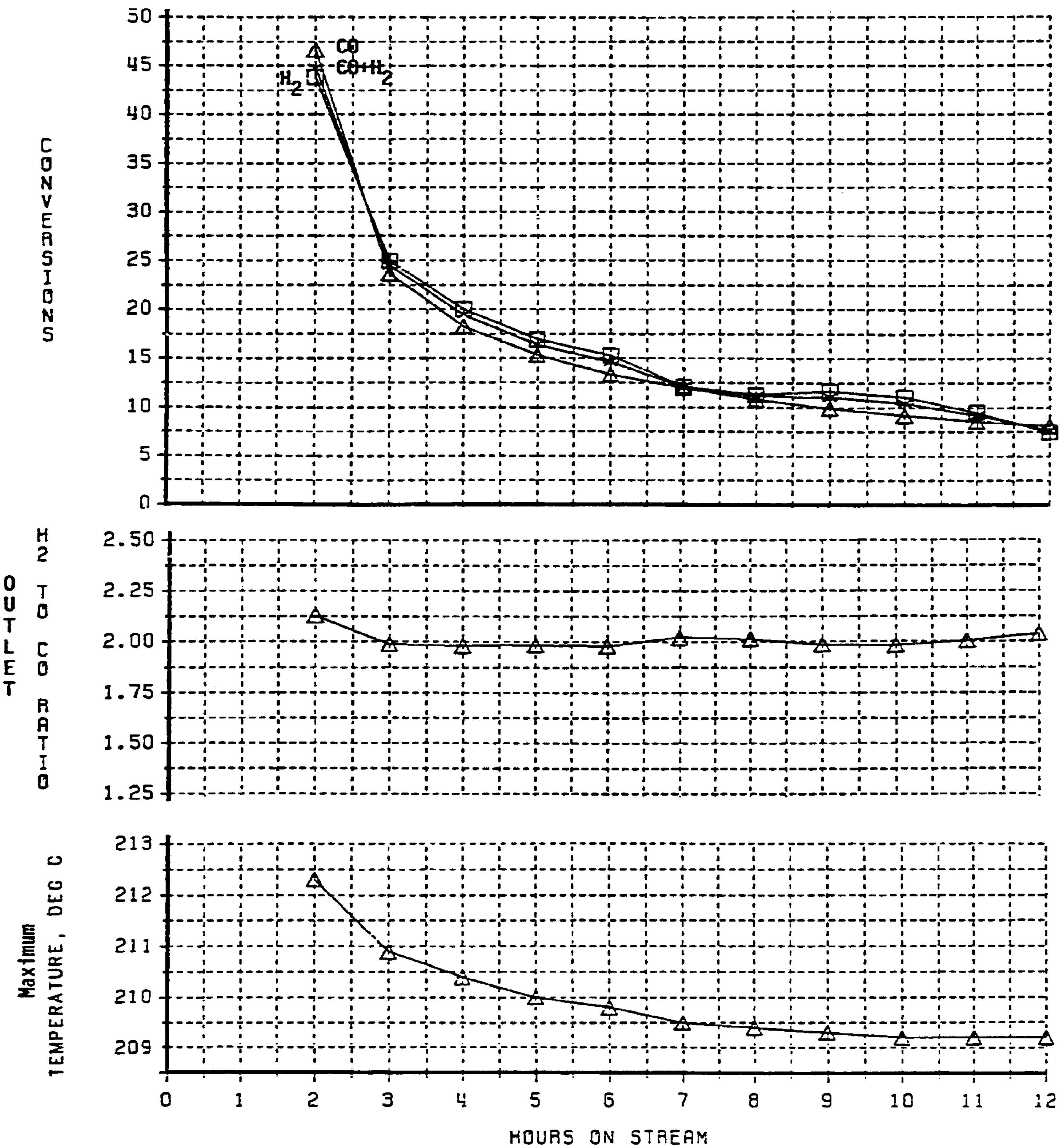

Figure 5-221. Titania-Supported Highly Dispersed Ruthenium Catalyst 5345-61: Water Gas Shift Activity in Run 30 (H_2:CO Feed Ratio = 2.0; 208°C at Inlet, 35 atm)

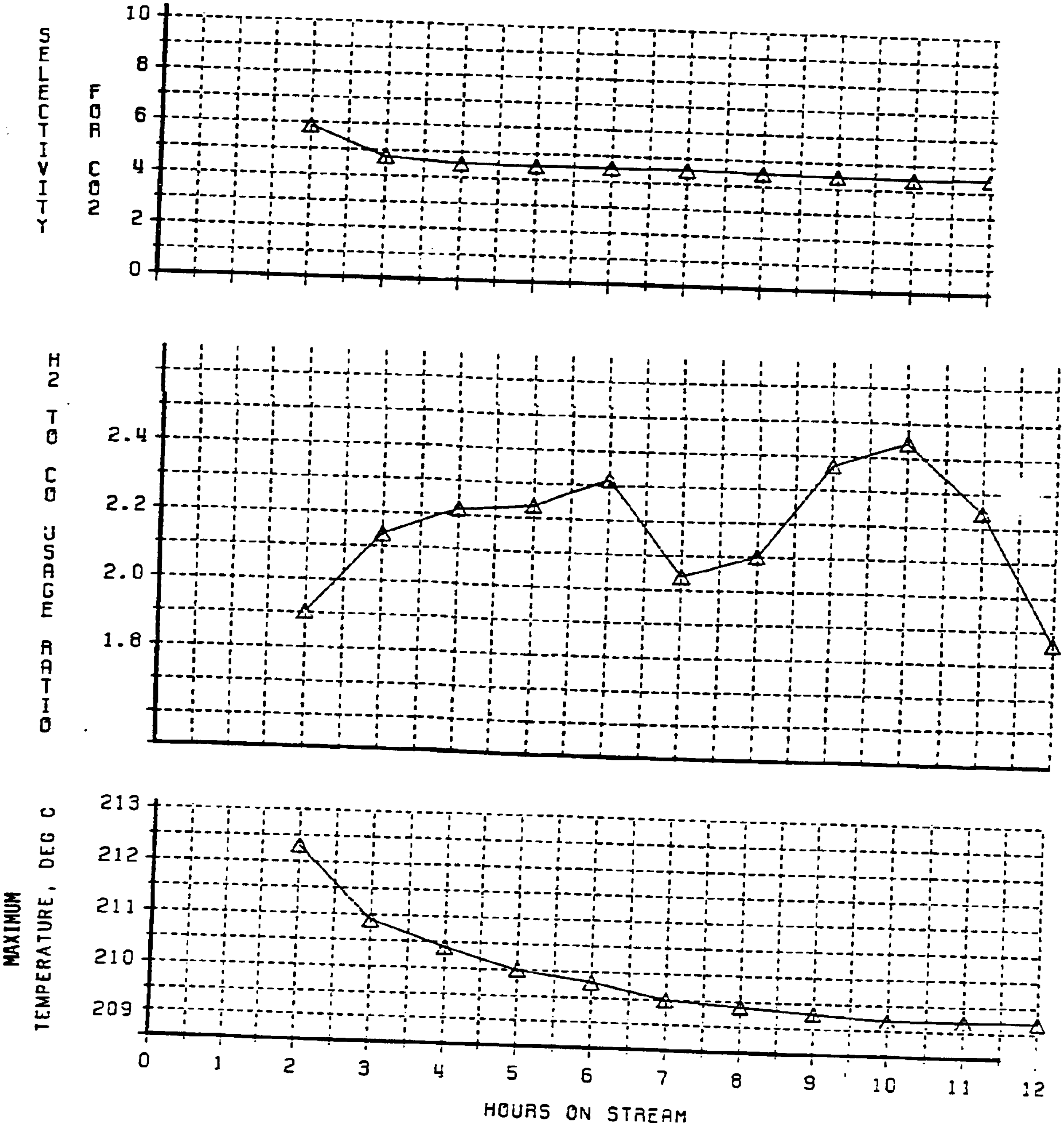

Figure 5-222. Titania-Supported Highly Dispersed Ruthenium Catalyst 5345-61:C_1 and C_2 Selectivities in Run 30 (H_2:CO Feed Ratio = 2.0, 208°C at Inlet, 35 atm)

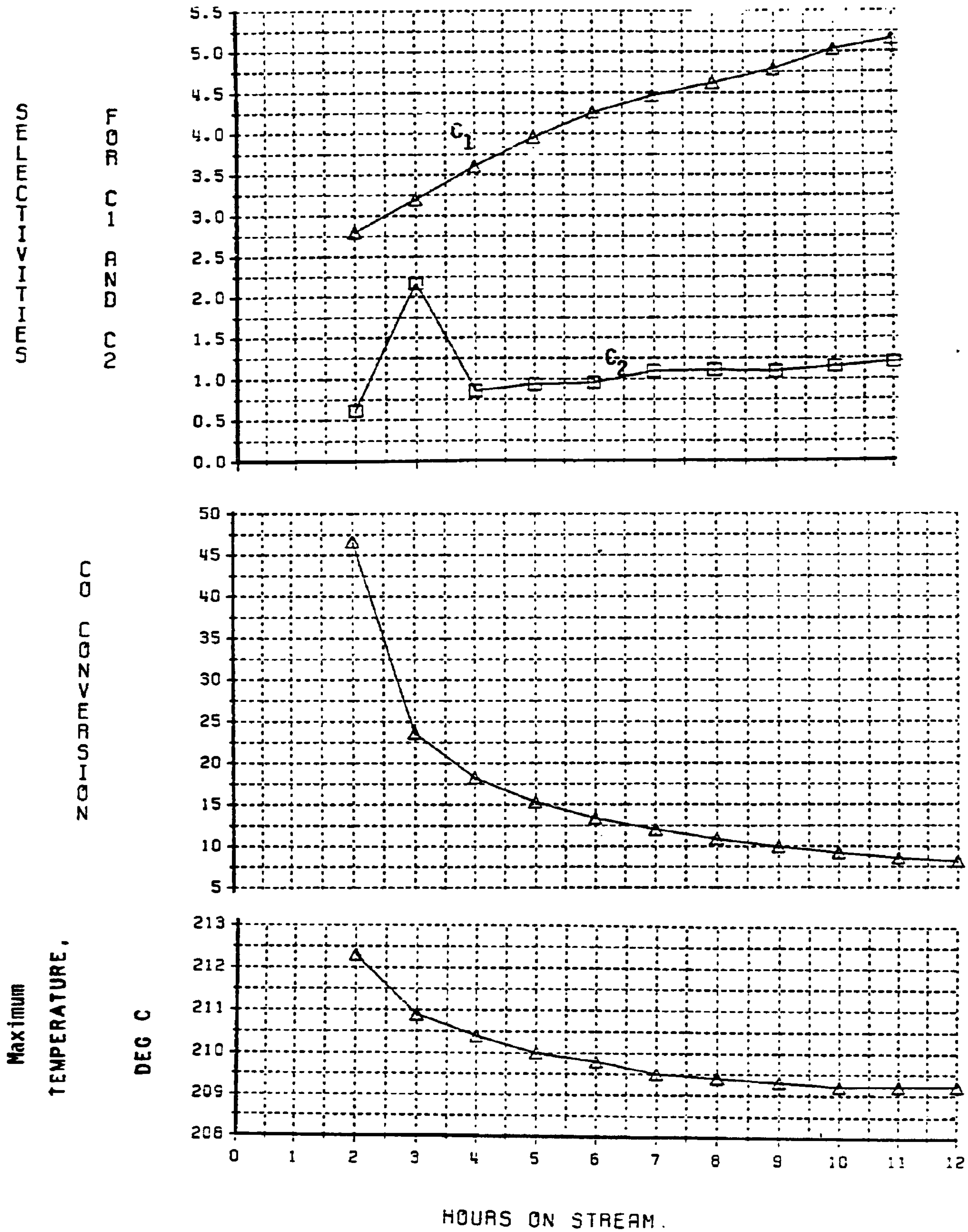

Figure 5-223. Titania-Supported Highly Dispersed Ruthenium Catalyst 5345-61: C_3 and C_4 Selectivities in Run 30 (H_2:CO Feed Ratio = 2.0, 208°C at Inlet, 35 atm)

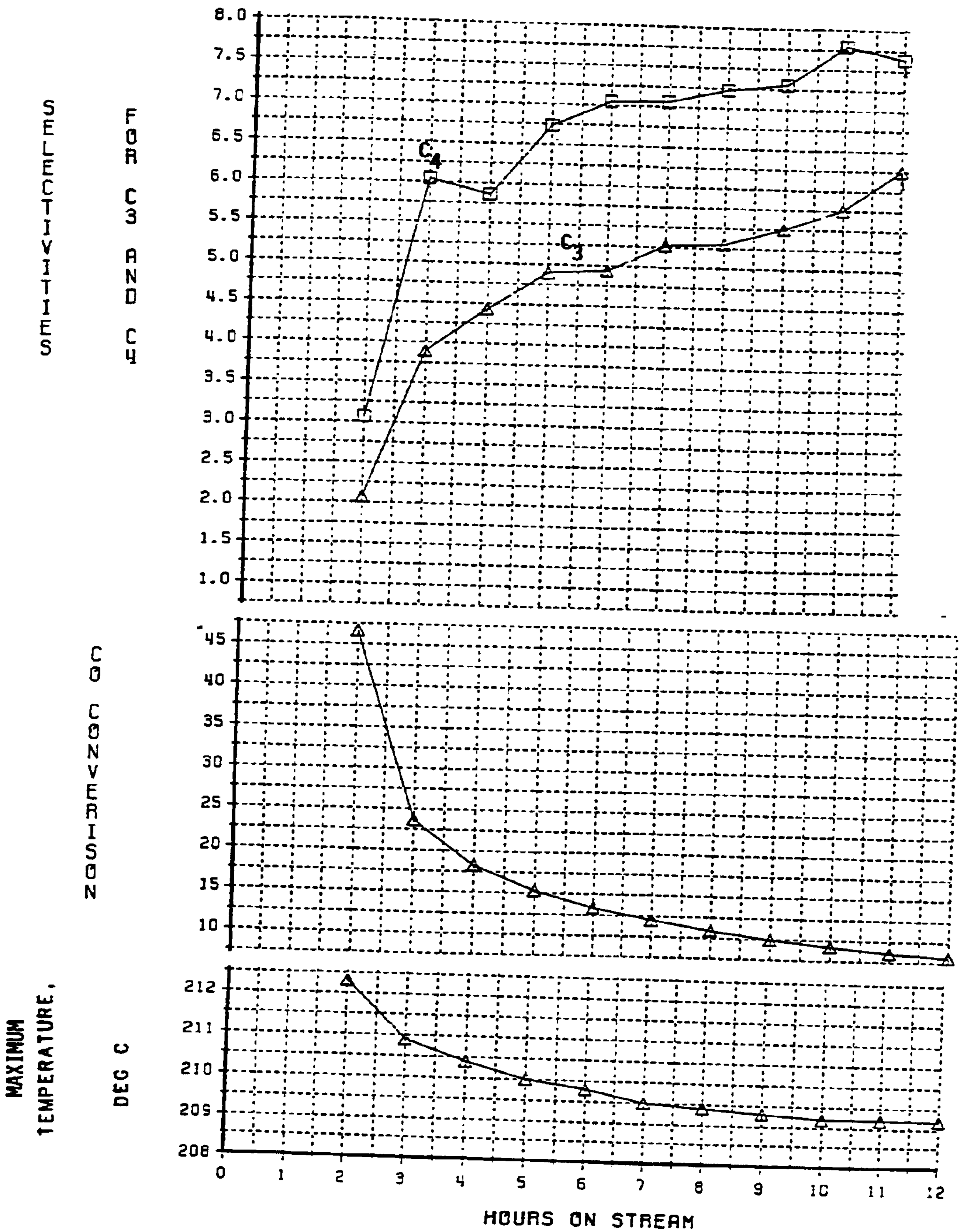

Figure 5-224. Titania-Supported Highly Dispersed Ruthenium Catalyst 5345-61: Olefin:Paraffin Ratios in Run 30 (H_2:CO Feed Ratio = 2.0, 208°C at Inlet, 35 atm)

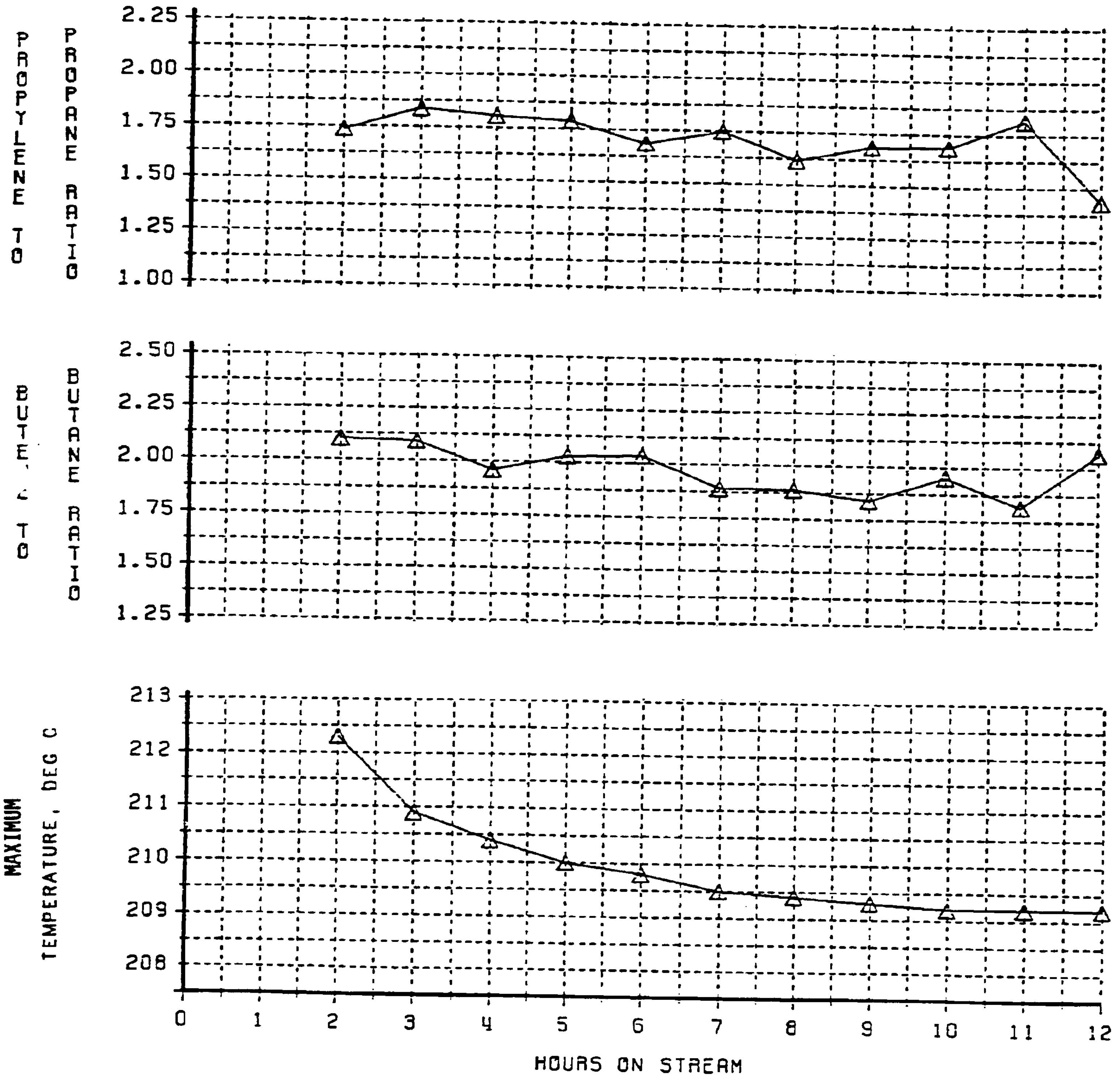

Figure 5-225. Anderson-Schulz-Flory Distribution with Titania-Supported Highly Dispersed Ruthenium Catalyst 5345-61 in Run 30 (Hydrocarbons only; C_1-C_{44})

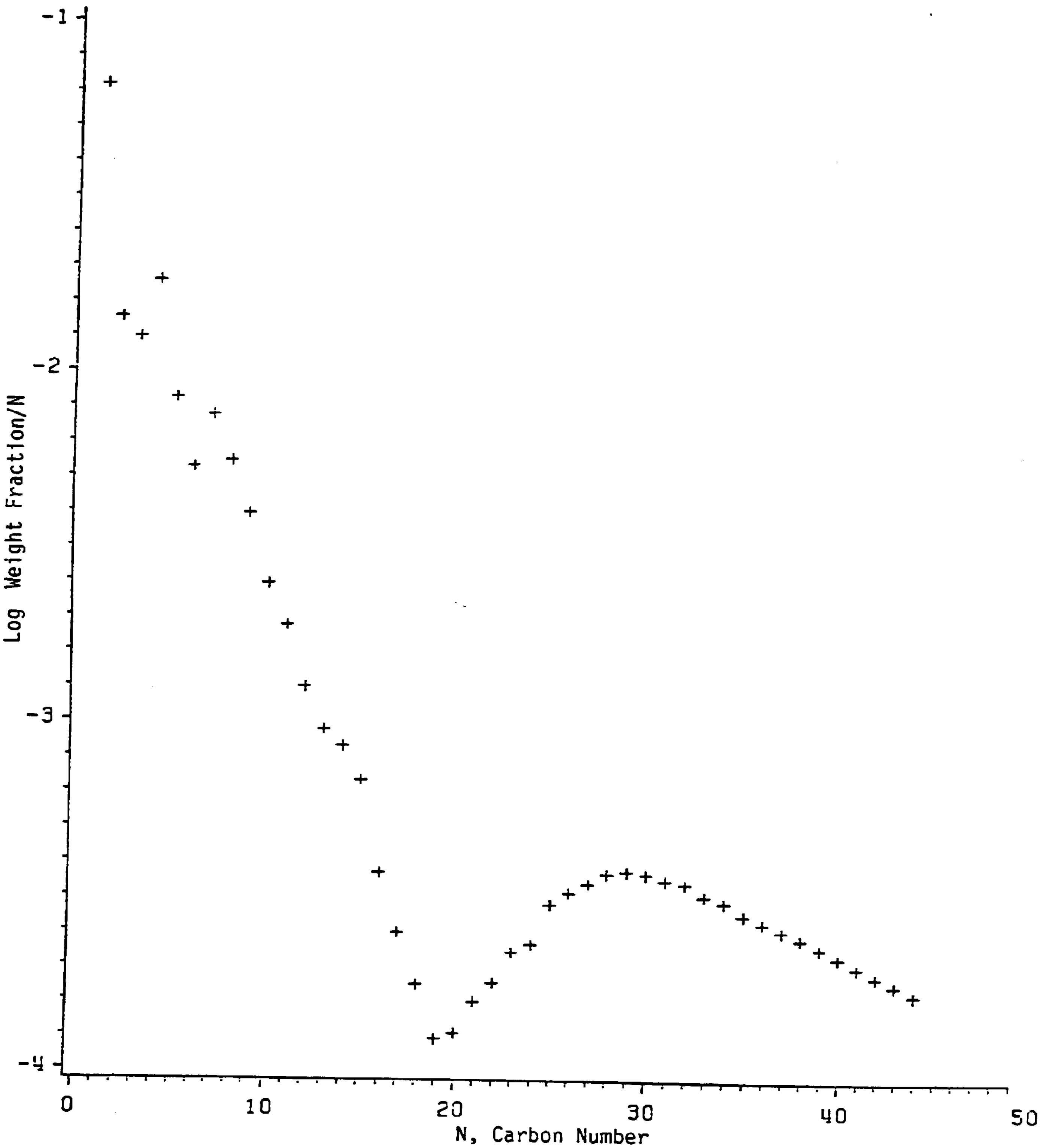

Figure 5-226. Anderson-Schulz-Flory Distribution with Titania-Supported Highly Dispersed Ruthenium Catalyst 5345-61 in Run 30 (Hydrocarbons only; C_1-C_{250})

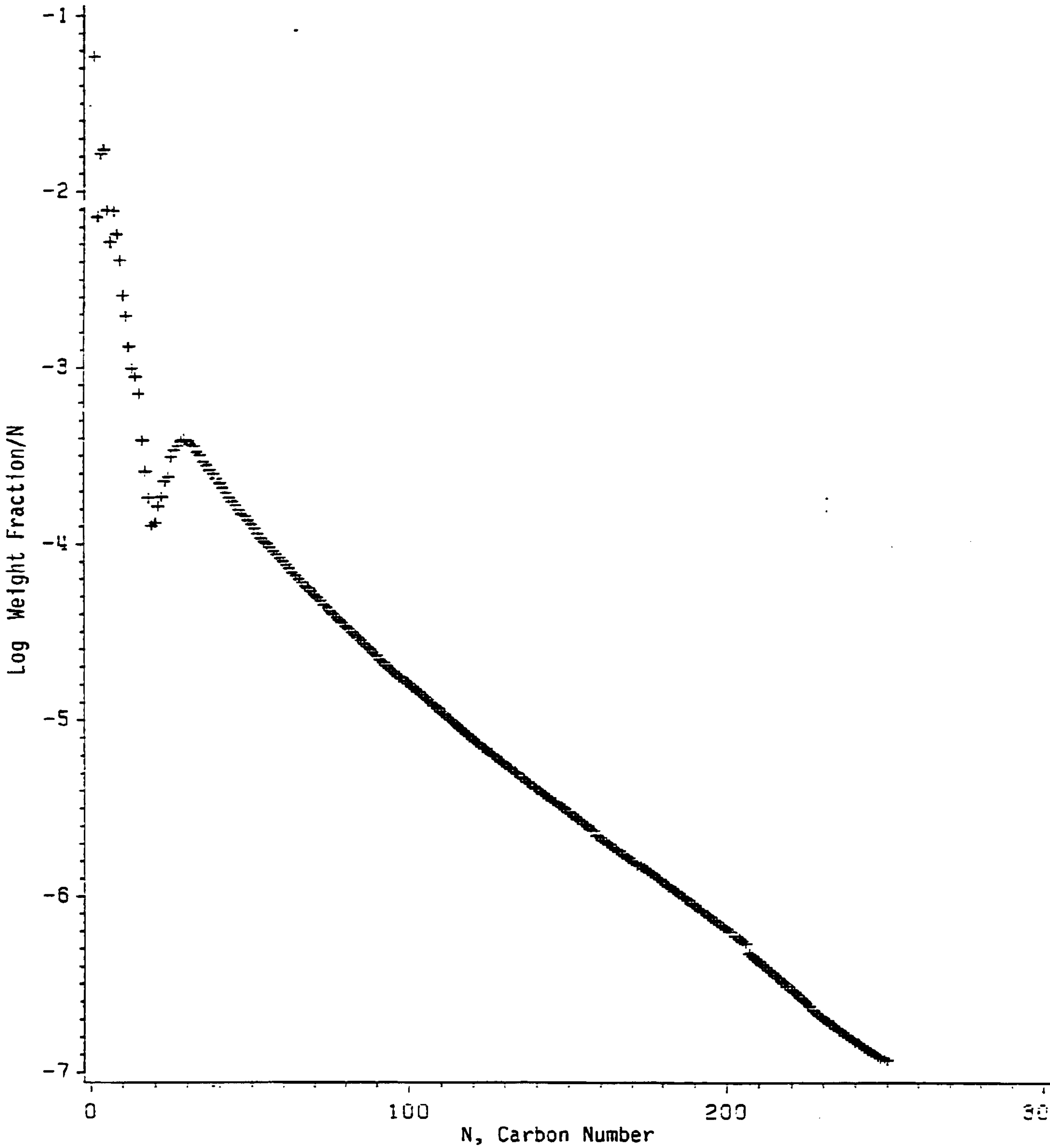

which was also apparent from the H_2:CO usage ratio which was mostly higher than 2 (Figure 5-221). This result is in contrast with highly dispersed ruthenium on alumina which was active for the water gas shift reaction. The olefin to paraffin ratios were higher than those obtained with alumina-supported highly dispersed catalyst.

C_6-C_{28} products were not recovered fully in the product receivers because of the short duration of the test. Nevertheless, 46% of the products were recovered from the used catalyst and showed an Anderson-Schulz-Flory distribution with $\alpha = 0.951$ at C_{30}-C_{70} and $\alpha = 0.968$ at C_{90}-C_{240}. It was, therefore, possible to conclude that cutoff did not occur with ruthenium particles which were smaller than 2 nm on titania.

As opposed to the alumina-supported highly dispersed ruthenium catalyst, there was no noticeable ruthenium metal agglomeration on the used titania-supported catalyst, according to STEM examination. Also, ruthenium carbonyl was not detected at the reactor outlet during testing of Catalyst 5345-61, and no Ru was lost during the test (Figure 5-227).

It is interesting to note that 1-5 nm ruthenium particles were observed during re-examination of the same STEM sample of the used Catalyst 5345-61 four months after the test. The STEM sample was exposed to air during this four-month period.

The causes for the enhanced stability of ruthenium on titania relative to on alumina may be explained by a stronger metal support interaction (SMSI) in the case of titania. The SMSI effect is also suggested by the higher oxygen uptake relative to the H_2 uptake observed with this catalyst. The low H_2 uptake on titania-supported reduced ruthenium after oxygen exposure may be explained by

Figure 5-227

STEM Micrographs of Well-Dispersed Ru/TiO_2 Catalyst

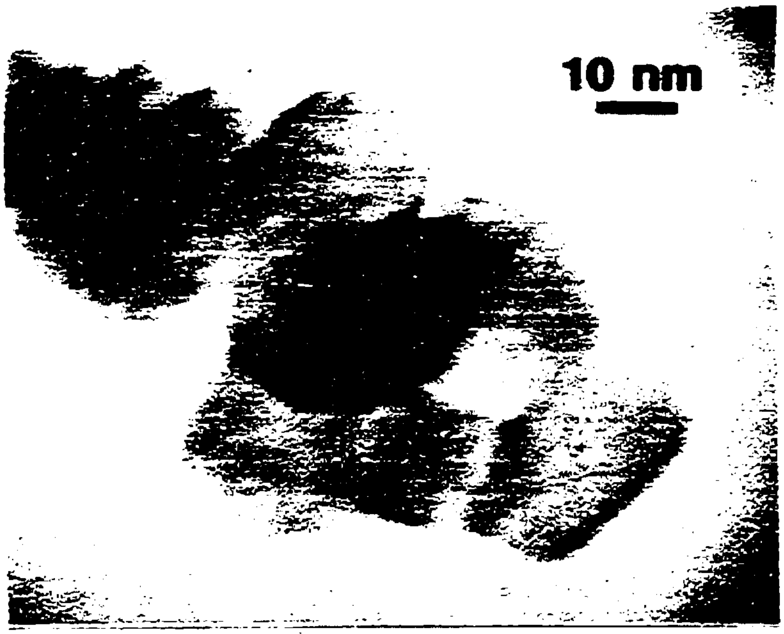

FRESH

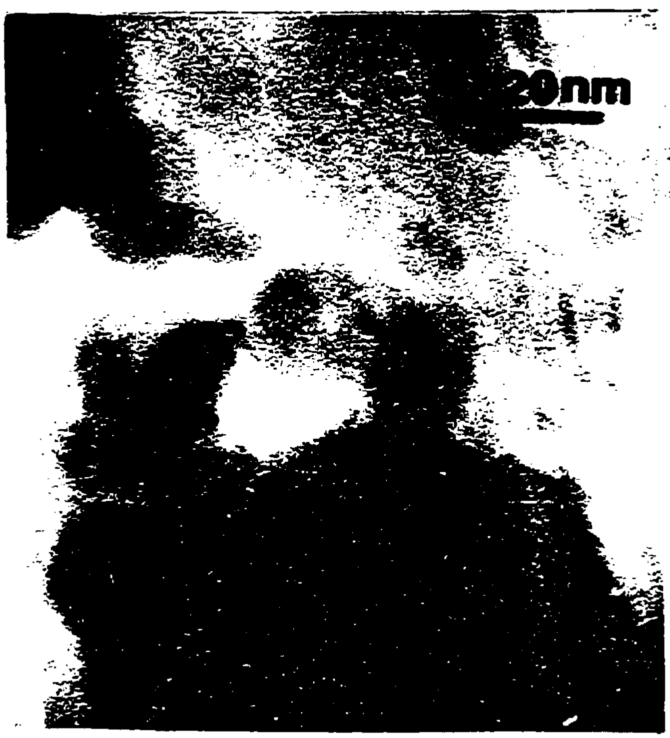

USED

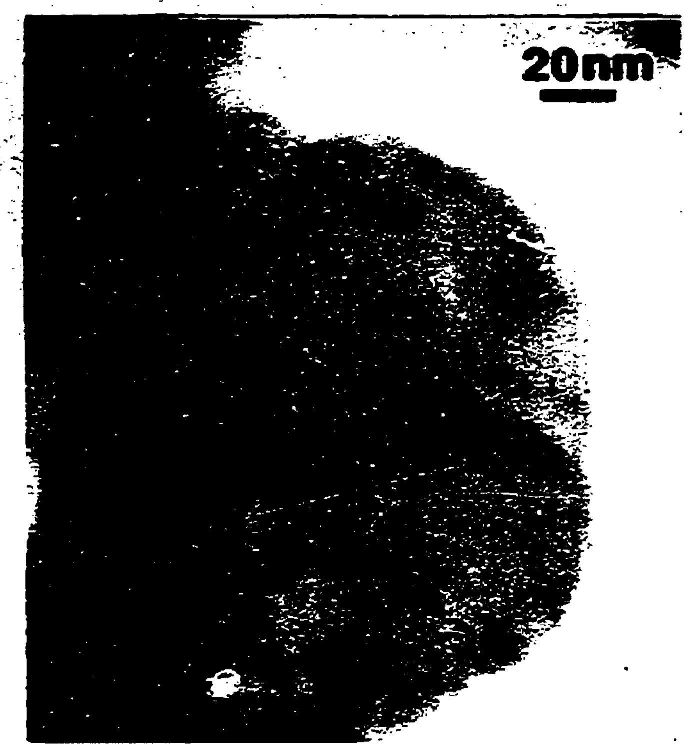

USED (After Air Exposure)

migration of a titania species over ruthenium. However, the possibility of ruthenium agglomeration after exposure of reduced ruthenium to oxygen cannot be discounted, particularly in view of the ruthenium agglomeration observed after air exposure of the STEM sample.

5.2.2.3 3-10 nm Ruthenium on Titania

Catalyst 4966-106 was prepared by the reverse micelle technique on the same titania support that was used for preparing Catalyst 5345-61 with highly dispersed ruthenium. The finished catalyst had 3-10 nm ruthenium particles according to STEM examination and was tested in Run 31 in an attempt to learn about ruthenium particle size effects on titania. The test conditions were the same as in Run 30 with highly dispersed ruthenium catalyst: H_2:CO feed ratio = 2, 208°C at inlet, 35 atm, 460 GHSV (Figures 5-228 through 5-231).

The high temperature H_2 pretreatment in Run 31 was conducted in the same manner as in Run 30. The initial CO conversion was 12% and declined to 3% by the end of 5 hours, after which the gas hourly space velocity was lowered to 170 hr^{-1}. This raised the CO conversion to 9-10% (Figure 5-228). At the same space velocity, the conversions obtained with Catalyst 4966-106 having 3-10 nm ruthenium particles on titania were much lower than those obtained under the same test conditions with Catalyst 5345-61 having highly dispersed ruthenium on titania. The catalyst with larger ruthenium particles showed higher CO_2 selectivity throughout the entire run relative to the catalyst with highly dispersed ruthenium (Figure 5-229), which is opposite to what was observed with alumina-supported catalysts. There was no obvious difference in selectivities to C_2, C_3 and C_4 hydrocarbons in Runs 30 and 31, while the selectivity to methane was lower with the catalyst having larger ruthenium particles.

Figure 5-228. Titania-Supported Catalyst 4966-106 with 3-10 nm Ruthenium Particles: Conversions in Run 31 (H_2:CO Feed Ratio = 2.0, 208°C at Inlet, 35 atm)

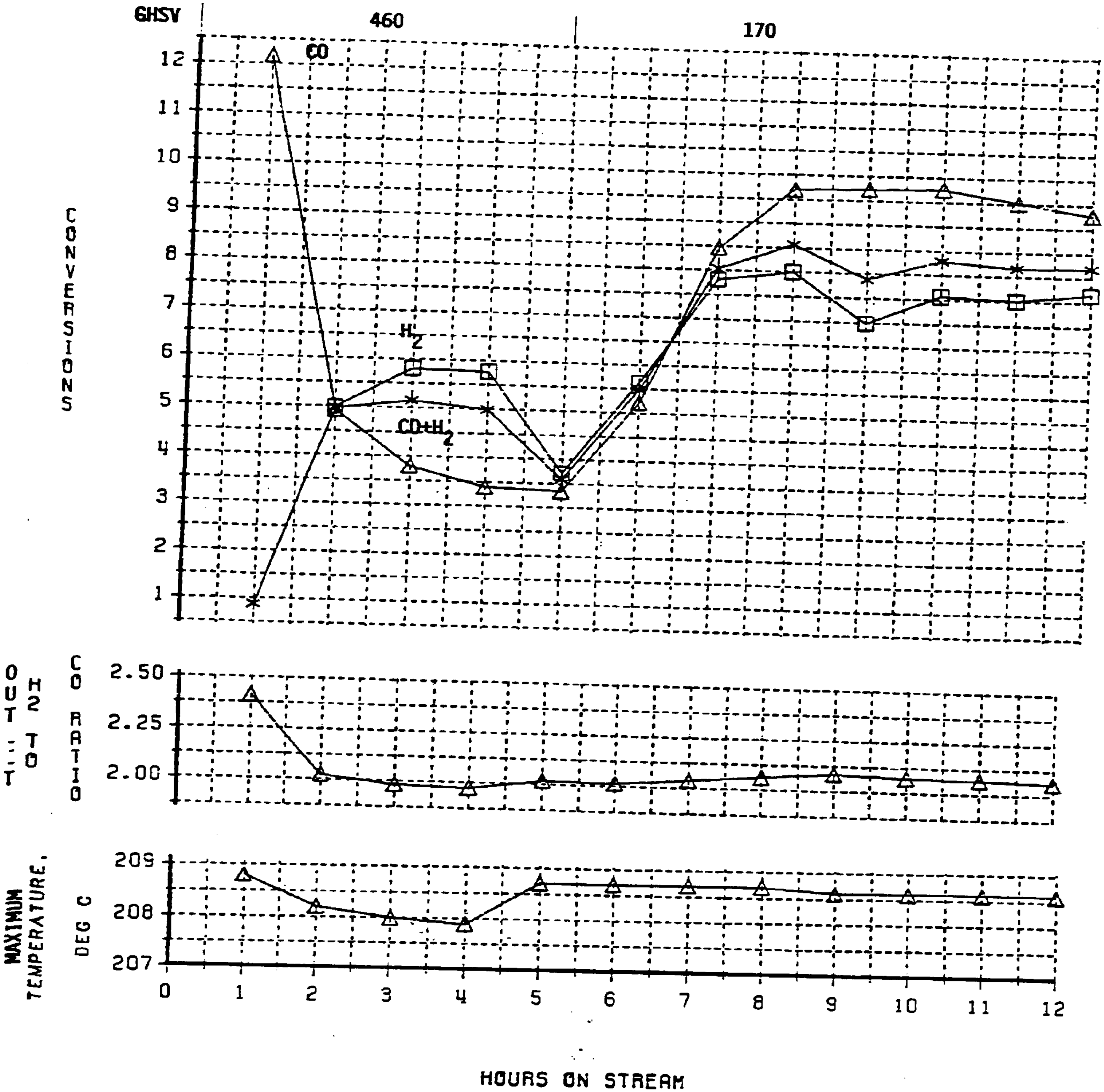

Figure 5-229. Titania-Supported Catalyst 4966-106 with 3-10 nm Ruthenium Particles: Water Gas Shift Activity in Run 31 (H_2:CO Feed Ratio = 2.0, 208°C at Inlet, 35 atm)

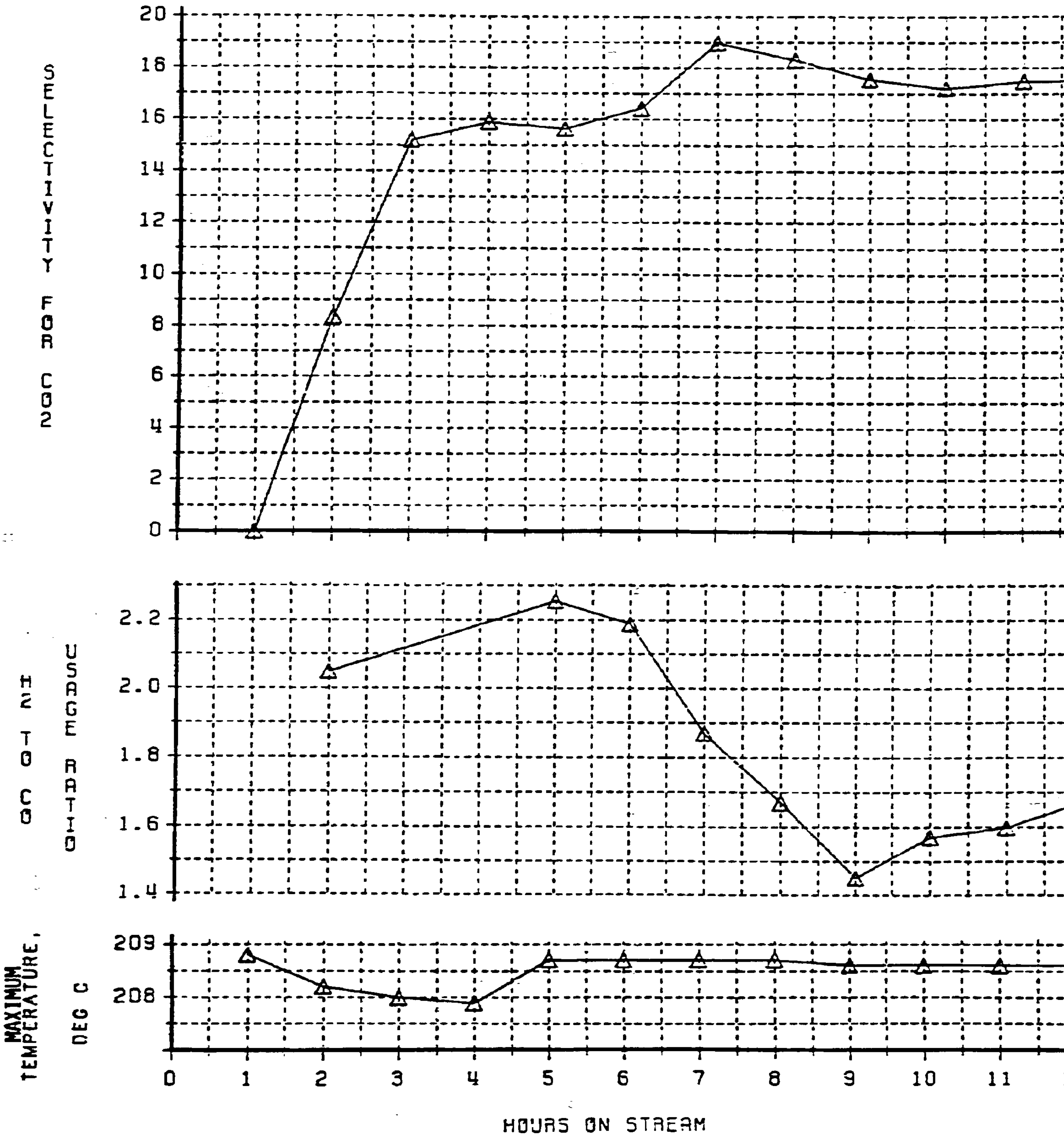

Figure 5-230. Titania-Supported Catalyst 4966-106 with 3-10 nm Ruthenium Particles: C_1-C_4 Selectivities in Run 31 (H_2:CO Feed Ratio = 2.0, 208°C at Inlet, 35 atm)

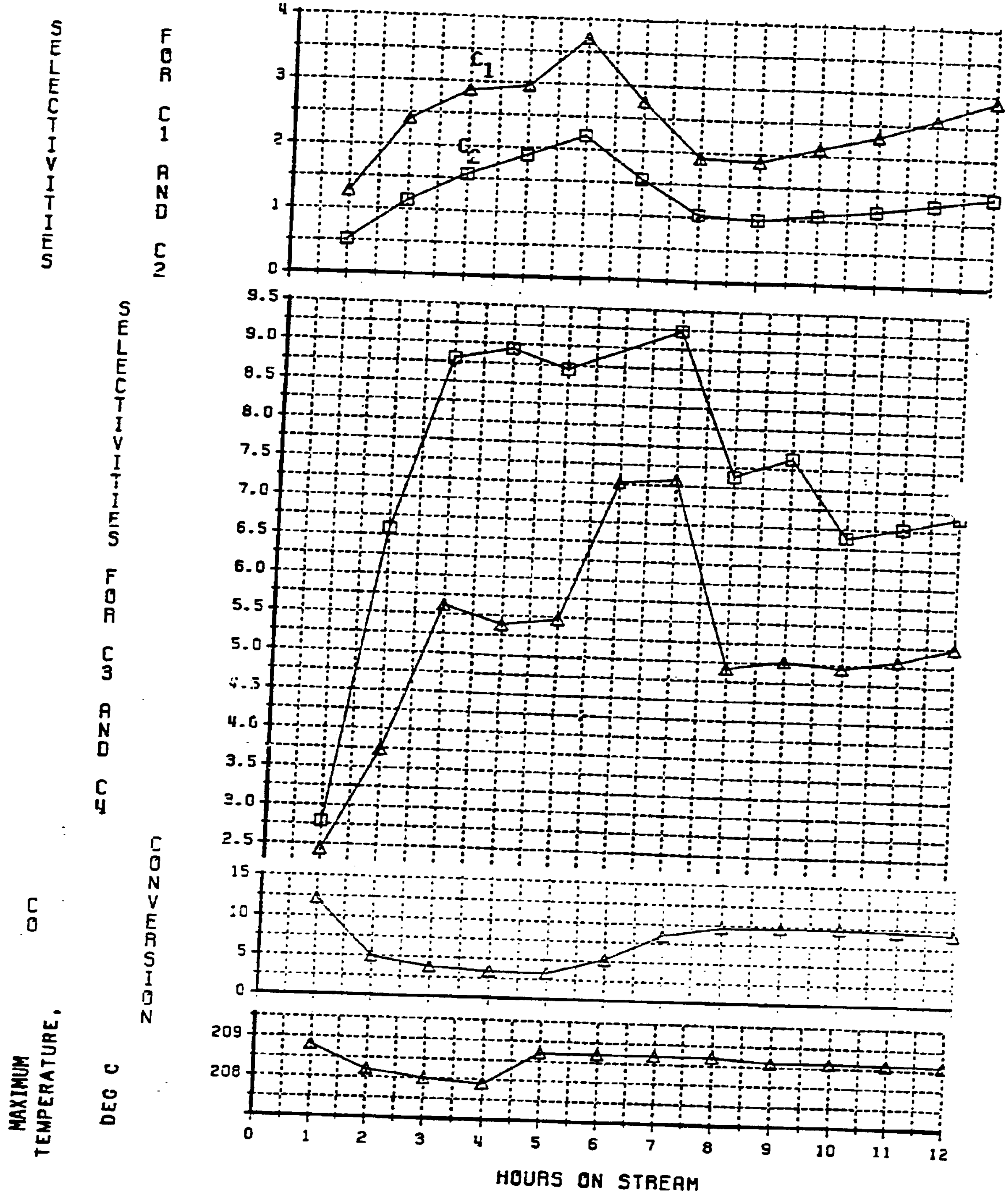

Figure 5-231. Titania-Supported Catalyst 4966-106 with 3-10 nm Ruthenium Particles: Olefin:Paraffin Ratios in Run 31 (H_2:CO Feed Ratio = 2.0, 208°C at Inlet, 35 atm)